

# Influence of the procedure for determining the characteristic values of strength parameters on the probability of failure of unsupported cuts

## Influence de la procédure de détermination des valeurs caractéristiques des paramètres de résistance sur la probabilité de rupture des talus d'excavation

F.P.S. Rogério\*

*DEC/ISPTundavala, Lubango, Angola. NOVA School of Science and Technology, Almada, Portugal*

N.M.C. Guerra, A.N. Antão, M. Vicente da Silva

*UNIC, NOVA School of Science and Technology, Almada, Portugal*

M. Matos Fernandes

*FEUP, Porto, Portugal*

*\*f.rogerio@campus.fct.unl.pt*

**ABSTRACT:** Estimating the characteristic value of strength parameters for design is an important matter in geotechnical practice. In this study, Latin Hypercube Sampling (LHS) is used to generate statistical meshes with the spatial variability of the friction angle and the true effective cohesion of the soil. For this, typical values of the coefficient of variation and of the horizontal and vertical scales of fluctuation of the friction angle and of the effective cohesion are adopted. Soil characterization is simulated in each of these statistical meshes. The characteristic values of the friction angle and effective cohesion are estimated following two procedures regarding the assumed knowledge of the soil properties. With these characteristic values, unsupported cuts are designed using the Load and Resistance Factor Design (LRFD) method. Slope stability analyses are performed with the software *mechpy*, using the Random Finite Element Limit Analysis (RFELA) and considering the above-mentioned meshes. Then, the probability of failure of the designed unsupported cuts is estimated using direct reliability analysis. The results show that adopting this procedure using simulation of site characterization has a substantial effect on the probability of failure.

**RÉSUMÉ:** L'estimation de la valeur caractéristique des paramètres de résistance pour le projet est une question importante pour la pratique géotechnique. Dans cette étude, l'échantillonnage hypercube latin (LHS) est utilisée pour générer des mailles statistiques avec la variabilité spatiale de l'angle de frottement et de la cohésion effective réelle du sol. Des valeurs typiques du coefficient de variation et des échelles horizontale et verticale de fluctuation sont adoptées pour caractériser le sol. Les valeurs caractéristiques de l'angle de frottement et de la cohésion effective sont estimés en suivant deux procédures en fonction de la connaissance supposée des propriétés du sol. Les talus d'excavation sont dimensionnés en utilisant la méthode *Load and Resistance Factor Design* (LRFD). Les analyses de stabilité des talus sont réalisées en utilisant le logiciel *mechpy* et le *Random Finite Element Limit Analysis* (RFELA) en prenant en compte les maillages statistiques. Enfin, la probabilité de rupture des talus d'excavation non soutenus est estimée à l'aide d'une analyse de fiabilité directe. Les résultats montrent que l'adoption de cette procédure utilisant la simulation de la caractérisation du site a un effet substantiel sur la probabilité de rupture.

**Keywords:** Characteristic value; simulated characterization; unsupported cut; probabilistic analysis; numerical limit analysis.

## 1 INTRODUCTION

The load and resistance factor design (LRFD) method uses representative values that can be taken as characteristic values, determined from the available data of soil characterization using statistical methods. When performing probabilistic analyses, it is important to take into account the spatial variability

of soil properties to properly account for the inherent uncertainties, as it was shown in several studies that spatial variability has a significant effect on the probability of failure (Cho, 2007; Griffiths et al., 2009; Ji et al., 2012; Chok et al., 2015; Yang et al., 2022). The main objective of this study is to assess the influence of the procedure used for determining

the characteristic values of the effective cohesion,  $c'$ , and the friction angle,  $\phi'$ , of soil on the probabilistic analysis of unsupported cuts under drained conditions, considering the effect of spatial variability. An adaptation of the Random Finite Element Method (RFEM) (Fenton & Griffiths, 2008), the Random Finite Element Limit Analysis (RFELA) is used for this purpose. A similar procedure can be applied to undrained conditions.

Latin Hypercube Sampling (LHS) is used to generate statistical meshes with the spatial variability of  $c'$ , and  $\phi'$  of soil in drained conditions, adopting typical values of the coefficient of variation, COV, and of the scales of fluctuation in the horizontal and vertical directions,  $\theta_x$ , and  $\theta_y$  (Phoon & Kulhawy, 1999; Cami et al., 2020; ISSMGE-TC304, 2021).

The characteristic values of the strength parameters are estimated through two scenarios regarding the knowledge of the soil properties. One where there's no prior knowledge of the mean value and COV of the soil properties, and the other where there's prior knowledge of these soil parameters. The first scenario is based on a site characterization simulated on the statistical meshes. Then, the characteristic value for each statistical mesh is estimated from the mean value and COV of  $c'$  and  $\phi'$  therein obtained. In the second scenario, the characteristic value is estimated using the input parameters, the mean value, and the COV of  $c'$  and  $\phi'$  used to generate the statistical meshes. The properties' design values are defined according to the principles of the Eurocode 7. The unsupported cuts are designed using deterministic stability analyses with Finite Element Limit Analysis (FELA). These stability analyses aim to evaluate the maximum unit weight  $\gamma_{EC7}$  for which the unsupported cuts with height  $h$  and inclination  $\beta$  verify safety.

The stability analyses of the designed unsupported cuts are then evaluated with RFELA. The probability of failure is estimated through the direct integration of the Probability Density Function (PDF) on the failure side of the limit state function (Huang & Griffiths, 2011). The limit state function is defined by the margin of safety, computed by the difference between the resistance and the loading (Baecher & Christian, 2003; Christian, 2004).

The generation of the statistical meshes, the simulation of site investigation, and the stability analyses of unsupported cuts are performed using the software *mechpy* (Vicente da Silva & Antão, 2013), developed at the Department of Civil Engineering of NOVA School of Science and Technology. This is a FELA software, where the kinematic and static theorems of limit analysis are implemented within a

finite element analysis framework (Vicente da Silva et al., 2020). It has been applied by the authors to reliability analyses (Simões et al., 2014, 2020). The software uses a remesh procedure based on Martin's (2011) work. In this approach, the analyses are performed in 4 steps, in which the finite element meshes are progressively refined in the zones of higher plastic distortion.

## 2 DESCRIPTION OF THE PROBLEM

This paper considers a problem of an unsupported cut with  $h = 15$  m,  $l = 12$  m,  $L = 35$  m,  $L_1 = 50$  m,  $D = 22$  m, and  $\beta = 45^\circ$ , modelled in plane strain state, with the boundary conditions presented in Figure 1.

The shear strength parameters  $c'$  and  $\tan\phi'$  (here regarded as uncorrelated random variables) with the mean values of 10 kPa and  $27^\circ$ , and COV of 0.2 and 0.08, respectively, are assumed to follow the lognormal distribution, with the scales of fluctuation  $\theta_x$  (30, 50, 80, and  $\infty$ ) and  $\theta_y$  (1, 3, 80, and  $\infty$ ), measured in meters. Hence, four cases are assessed, three of which with spatial variability [case 1 ( $\theta_x = 30$  m;  $\theta_y = 1$  m); case 2 ( $\theta_x = 50$  m;  $\theta_y = 3$  m); case 3 ( $\theta_x = 80$  m,  $\theta_y = 80$  m)], and one without spatial variability [case 4 ( $\theta \rightarrow \infty$ )].

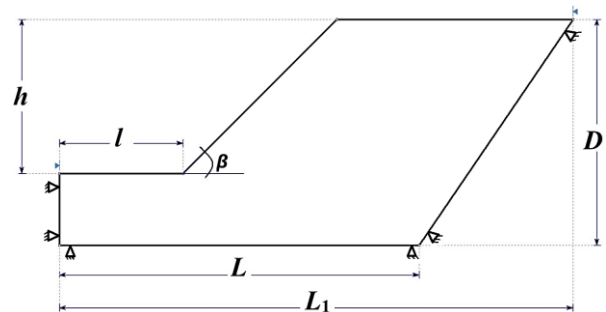


Figure 1. Geometry and boundary conditions of the numerical model.

The same values of scales of fluctuation are adopted for both  $c'$  and  $\phi'$ . Cases 1 and 2 correspond to realistic situations, whereas case 3 is used for control and comparison with case 4. For cases 3 and 4, only the second scenario is considered.

## 3 GENERATION OF STATISTICAL MESHES

The generation of the random fields is achieved with LHS, a more efficient sampling technique than standard Monte Carlo (McKay et al., 1979;

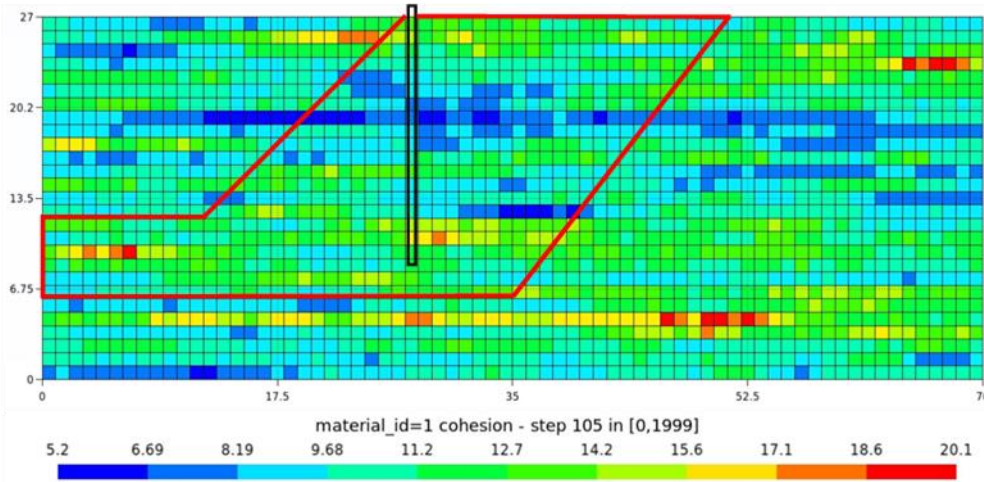


Figure 2. Example of a statistical mesh sample, of  $c'$  distribution, superposed with the geometry considered in finite element calculations.

Olsson et al., 2003). A two-dimensional ellipsoidal correlation function is used to describe the autocorrelation of the random variables (Fenton & Griffiths, 2008), from element to element, for a horizontal distance,  $\Delta_x$ , and a vertical distance,  $\Delta_y$ , from the centre of mass for the elements of the statistical mesh:

$$\rho(\Delta x, \Delta y) = \exp \left[ -2 \sqrt{\left( \frac{\Delta x}{\theta_x} \right)^2 + \left( \frac{\Delta y}{\theta_y} \right)^2} \right] \quad (1)$$

in which  $\rho$  is the coefficient of correlation. An example of a statistical mesh is presented in Figure 2, with 70 m width and 27 m height, containing square statistical elements of  $1 \times 1 \text{ m}^2$  dimension. For this study, 2000 statistical meshes were generated for each of the cases 1 to 3 described in section 2.

#### 4 SITE CHARACTERIZATION

The site characterization is simulated on both  $c'$  and  $\phi'$  statistical meshes and provides the “exact” value of these spatially distributed random properties, although, in practice, measurement errors are inevitable (Yang et al., 2022). This simulation of site investigation is executed at the crest of the unsupported cut as shown in Figure 2 obtaining the values of  $c'$  and  $\phi'$ , from the top boundary down to  $1.2h$ . In this procedure, these values are collected at points situated 1 m from each other, assuming that such values could be obtained from site characterization, for each statistical mesh. The values of  $c'$  and  $\phi'$  obtained in this way are used for determining the characteristic values of the parameters, for each sample, for the 1<sup>st</sup> scenario described in Section 1. In this scenario, 2000

characteristic values are calculated for each case, while in the 2nd scenario, only one characteristic value is computed for each case.

#### 5 DESIGN

The characteristic value is defined from the values of the parameters of the statistical meshes using the following equation:

$$X_k = \exp[Y_m(1 - k_n \cdot COV_{\ln X})] \quad (2)$$

where  $Y_m$  is the mean value of the logarithms of individual parameters, and  $k_n$  is the statistical coefficient related to the type of distribution, confidence limit, and number of test values  $n$ . For the first scenario,  $k_n$  is calculated using the expression:

$$k_n = t_{n-1}^{0.95} \sqrt{1/n} \quad (3)$$

in which  $t_{n-1}^{0.95}$  is the student's t-value for  $n-1$  degrees of freedom at a confidence level of 95% (Bond & Harris, 2006; Frank et al., 2004). In this scenario,  $n = 19$ , which corresponds to the number of values of  $c'$  and  $\phi'$  collected in each characterization simulated.

As for the second scenario,  $k_n$  is estimated by:

$$k_n = N_{95} \sqrt{1/n} \quad (4)$$

where  $N_{95}$  represents the Normal distribution, evaluated for a 95% confidence level and infinite degrees of freedom. For this scenario,  $k_n$  is computed by assuming  $n = 30$ .

The design value of the ground properties  $X_d$  is derived from the characteristic value by applying the Design Approach 1, Combination 2 (DA1 – C2) of the Eurocode 7 (EN 1997-1, 2004),

$$X_d = x_k/\gamma_M \quad (5)$$

in which  $\gamma_M$  is the partial factor of safety considered equal to 1.25 for  $c'$  and  $\tan\phi'$ .

## 6 STABILITY ANALYSIS

This process starts by mapping the values of  $c'$  and  $\phi'$  from the statistical meshes into the finite element mesh with the geometry of the unsupported cut (Figure 2), as presented in the example in Figure 3 a). Subsequently, the stability analyses are performed, applying the kinematic and static theorems of limit analysis. The approximation of the unit weight that causes the collapse of the unsupported cut is obtained from both analyses and the average of the two,  $\gamma_{RFELA,i}$ , is determined for each statistical mesh sample. The failure mechanisms can be inferred from the mesh deformation and the maximum distortion (Figure 3 b)) in the case of the kinematic theorem calculations.

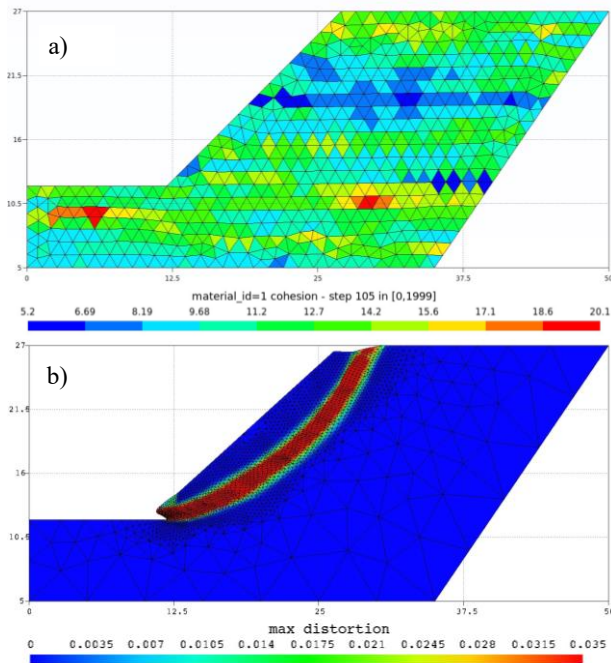


Figure 3. Example of a result of: a) mapping RFELA mesh values of  $c'$ , and b) a deformed mesh with maximum distortion, determined from kinematic theorem calculations.

## 7 PROBABILITY OF FAILURE

For performing the direct reliability analysis, in this study, the margin of safety is computed as:

$$M = \gamma_{RFELA} - \gamma_{EC7} \cdot (1 + COV \cdot \Delta) \quad (6)$$

in which  $\Delta$  is either zero or a random “noise” that follows the normal standard distribution, with a mean of 0 and a standard deviation of 1, assuming that COV is equal to 0.10. The implementation of the random “noise” seeks to simulate the effect of variability in the action.

The purpose is to find the probability of  $M \leq 0$ , and it is estimated using the cumulative distribution function of either the Normal or the Log-normal distribution.

For cases 1 and 2 it was found that the Normal distribution gave the best approximation to the data, and for cases 3 and 4 it was the Log-normal.

Figure 4 presents an example of the CDF of the margin of safety, for comparison of a situation with the random “noise” ( $M\Delta \rightarrow \Delta \neq 0$ ) and another without it ( $M \rightarrow \Delta = 0$ ). It is also possible to observe that the random “noise” has a significant effect on the probability of failure.

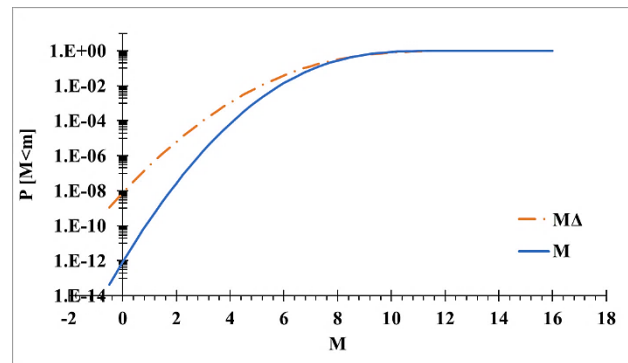


Figure 4. Cumulative distribution function of the margin of safety for case 1, with site characterization simulation.

Table 1 lists the results of the cases considered in this study. It shows that the probability of failure increases with the scale of fluctuation. There are clear differences in the results of the first ( $1^{st}$  sc.) and the second ( $2^{nd}$  sc.) scenarios considered. The probability of failure is substantially lower in the first scenario in both cases 1 and 2. The difference between the two scenarios is much greater when no random “noise” is considered.

Figure 5 presents the comparison between the curves of the cumulative relative frequency of cases 1 and 2, for  $\Delta = 0$ ,  $1^{st}$  scenario. It shows how in the first case the values remain closer to the overall mean value of  $M$ , therefore with a lower probability of failure. This suggests that, with greater spatial variability (smaller  $\theta$ ), the mean values of ground properties along the slip surface in the generated statistical meshes are closer to its overall mean value. As the scale of fluctuation increases, the spatial distribution of ground properties approximates a

homogeneous state ( $\theta \rightarrow \infty$ ). Therefore, the mean values of the properties in the statistical meshes along the slip surface exhibit a growing divergence from the overall mean value. When the spatial variability of shear strength properties is not considered in probabilistic analysis, the probability of failure is considerably higher (case 4).

Table 1. Results of the probabilistic analyses.

Case	$\theta_x$ (m)	$\theta_y$ (m)	$P_f$			
			$\Delta = \theta^1$		$\Delta \neq \theta^2$	
			1 <sup>st</sup> sc. <sup>3</sup>	2 <sup>nd</sup> sc. <sup>4</sup>	1 <sup>st</sup> sc. <sup>3</sup>	2 <sup>nd</sup> sc. <sup>4</sup>
1 <sup>5</sup>	30	1	$8.4 \times 10^{-13}$	$2.2 \times 10^{-9}$	$8.3 \times 10^{-9}$	$3.8 \times 10^{-7}$
2 <sup>5</sup>	50	3	$5.8 \times 10^{-8}$	$3.4 \times 10^{-5}$	$2.0 \times 10^{-6}$	$1.2 \times 10^{-4}$
3 <sup>5</sup>	80	80	--	$3.0 \times 10^{-3}$	--	$4.6 \times 10^{-3}$
4 <sup>6</sup>	$\infty$	$\infty$	--	$2.7 \times 10^{-3}$	--	$4.5 \times 10^{-3}$

<sup>1</sup>without random noise; <sup>2</sup>with random noise; <sup>3</sup>first scenario; <sup>4</sup>second scenario; <sup>5</sup>RFELA analysis; <sup>6</sup>FELA analysis.

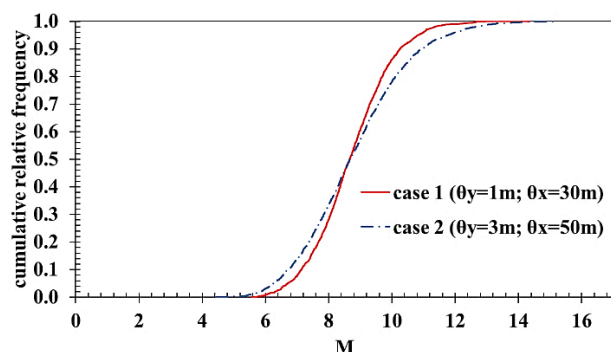


Figure 5. Example of the cumulative distribution function of the margin of safety, cases 1 and 2 (1<sup>st</sup> scenario;  $\Delta=0$ ).

When the scale of fluctuation is very high,  $\theta = 80$  m (case 3), the probability of failure is of the same order of magnitude as the analysis with  $\theta \rightarrow \infty$  (case 4). This is a consequence of the homogenization of the mesh caused by the low spatial variability.

These results demonstrate that when performing probabilistic analyses of unsupported cuts, it is important to consider the spatial variability of soil properties. It also shows the clear benefits of performing site characterization, for determining the characteristic value, rather than assuming complete knowledge of the grounds' properties, even in this case, where that knowledge was used to generate the samples themselves.

## 8 CONCLUSIONS

The degree of knowledge of a site's properties plays an important role in reliability analyses due to the influence of uncertainty on the probability of failure. The results show that the simulations of site characterization have a substantial effect on the

probability of failure; in every case studied it decreased the value obtained. The use of the characteristic values obtained from the simulated site characterization has emphasized its importance in the probabilistic analysis of unsupported cuts, even when there is prior knowledge of the ground properties.

Uncertainty in the actions has a major impact on the probability of failure, as its effect resulted in a clear reduction of its value for both scenarios.

Spatial variability of ground properties, within a realistic range, has a considerable influence on the probability of failure. Neglecting it can lead to an overestimation of the probability of failure.

The significance of the correlation between  $c'$  and  $\phi'$  in probabilistic analyses of unsupported cuts on spatially variable soils is an important aspect to ponder, and its effect is the subject of further study.

## ACKNOWLEDGEMENTS

The first author acknowledges the support from FCT through the PhD scholarship with reference PRT/BD/151571/2021.

## REFERENCES

- Baecher, G. B. and Christian, J. T. (2003). *Reliability and Statistics in Geotechnical Engineering*. John Wiley & Sons.  
<https://www.researchgate.net/publication/247385445>.
- Bond, A. and Harris, A. (2006). *Decoding Eurocode 7*. CRC Press. <https://doi.org/10.1201/9781482265873>
- Cami, B., Javankhoshdel, S., Phoon, K.-K. and Ching, J. (2020). Scale of Fluctuation for Spatially Varying Soils: Estimation Methods and Values. *ASCE-ASME Journal of Risk and Uncertainty in Engineering Systems, Part A: Civil Engineering*, 6(4), 03120002. <https://doi.org/10.1061/ajrua6.0001083>.
- Cho, S. E. (2007). Effects of spatial variability of soil properties on slope stability. *Engineering Geology*, 92(3-4), 97-109. <https://doi.org/10.1016/j.enggeo.2007.03.006>.
- Chok, Y. H., Jaksa, M. B., Griffiths, D. V., Fenton, G. A. and Kaggwa, W. S. (2015). Probabilistic analysis of a spatially variable  $c'-\phi'$  slope. *Australian Geomechanics Journal*, 50(2), 17-27. <http://random.engmath.dal.ca/fenton/pubs/journal/2015/>.
- Christian, J. T. (2004). Geotechnical Engineering Reliability: How Well Do We Know What We Are Doing? *Journal of Geotechnical and Geoenvironmental Engineering*, 130(10), 985-1003. [https://doi.org/10.1061/\(ASCE\)1090-0241\(2004\)130:10\(985\)](https://doi.org/10.1061/(ASCE)1090-0241(2004)130:10(985)).
- EN 1997-1. (2004). Eurocode 7: Geotechnical design - Part 1: General rules. CEN, European Committee for Standardization.

- Fenton, G. A. and Griffiths, D. V. (2008). *Risk assessment in geotechnical engineering*. John Wiley & Sons.
- Frank, R., Bauduin, C., Driscoll, R., Kavvas, M., Krebs Ovesen, N., Orr, T., Schuppener, B. and Gulvanessian H. (2004). Designers' guide to EN 1997-1 Eurocode 7: Geotechnical design - General rules. Thomas Telford. <https://www.icvirtuallibrary.com/doi/book/10.1680/dgte7.31548>.
- Griffiths, D. V., Huang, J. and Fenton, G. A. (2009). Influence of Spatial Variability on Slope Reliability Using 2-D Random Fields. *Journal of Geotechnical and Geoenvironmental Engineering*, 135(10), 1367–1378. [https://doi.org/10.1061/\(ASCE\)GT.1943-5606.0000099](https://doi.org/10.1061/(ASCE)GT.1943-5606.0000099).
- Huang, J. and Griffiths, D. V. (2011). Observations on FORM in a simple geomechanics example. *Structural Safety*, 33(1), 115–119. <https://doi.org/10.1016/j.strusafe.2010.10.001>
- ISSMGE-TC304. (2021). State of the art review of inherent variability and uncertainty in geotechnical properties and models. <http://140.112.12.21/issmge/tc304.htm?#6>.
- Ji, J., Liao, H. J. and Low, B. K. (2012). Modeling 2-D spatial variation in slope reliability analysis using interpolated autocorrelations. *Computers and Geotechnics*, 40, 135–146. <https://doi.org/10.1016/j.compgeo.2011.11.002>.
- Martin, C. M. (2011). The use of adaptive finite-element limit analysis to reveal slip-line fields. *Géotechnique Letters*, 1(2), 23–29. <https://doi.org/10.1680/geolett.11.00018>.
- McKay, M. D., Beckman, R. J. and Conover, W. J. (1979). Comparison of three methods for selecting values of input variables in the analysis of output from a computer code. *Technometrics*, 21(2), 239–245. <https://doi.org/10.1080/00401706.1979.10489755>.
- Olsson, A., Sandberg, G. and Dahlblom, O. (2003). On Latin hypercube sampling for structural reliability analysis. *Structural Safety*, 25(1), 47–68. [https://doi.org/10.1016/S0167-4730\(02\)00039-5](https://doi.org/10.1016/S0167-4730(02)00039-5).
- Phoon, K.-K. and Kulhawy, F. H. (1999). Characterization of geotechnical variability. *Canadian Geotechnical Journal*, 36(4), 612–624. <https://doi.org/https://doi.org/10.1139/t99-038>.
- Simões, J. T., Neves, L. C., Antão, A. N. and Guerra, N. M. C. (2014). Probabilistic analysis of bearing capacity of shallow foundations using three-dimensional limit analyses. *International Journal of Computational Methods*, 11(02), 1342008. <https://doi.org/10.1142/S0219876213420085>.
- Simões, J. T., Neves, L. C., Antão, A. N. and Guerra, N. M. C. (2020). Reliability assessment of shallow foundations on undrained soils considering soil spatial variability. *Computers and Geotechnics*, 119, 103369. <https://doi.org/10.1016/j.compgeo.2019.103369>.
- Vicente da Silva, M. and Antão, A. N. (2013). Programa mechpy. Available at: <http://geocluster.dec.fct.unl.pt/mechpy/>, accessed:22/10/2023.
- Vicente da Silva, M., Deusdado, N. and Antão, A. N. (2020). Lower and upper bound limit analysis via the alternating direction method of multipliers. *Computers and Geotechnics*, 124, 103571. <https://doi.org/10.1016/j.compgeo.2020.103571>.
- Yang, R., Huang, J. and Griffiths, D. V. (2022). Optimal geotechnical site investigations for slope reliability assessment considering measurement errors. *Engineering Geology*, 297. <https://doi.org/10.1016/j.enggeo.2021.106497>.